Anisotropic interaction of three-dimensional spatial screening solitons

A. Stepken and F. Kaiser

Institute of Applied Physics, Darmstadt University of Technology, Hochschulstrasse 4a, 64289 Darmstadt, Germany

M. R. Belić

Institute of Physics, P.O. Box 57, 11001 Belgrade, Yugoslavia

Received April 28, 1999; revised manuscript received August 2, 1999

A theory based on the paraxial propagation of laser beams in nonlinear media and on the Kukhtarev material equations is developed to explain the interaction of bright spatial screening solitons in photorefractive crystals. A numerical study in three dimensions is performed to reveal qualitative and quantitative agreement with experiment. Screening solitons display a variety of propagation effects, such as inelastic scattering, attraction and repulsion, and oscillation and spiraling. In particular, we investigate the influence of initial separation and launching directions on the propagation of incoherent solitons. © 2000 Optical Society of America [S0740-3224(00)00501-4]

OCIS codes: 190.5330, 190.5530.

1. INTRODUCTION

A great deal of research effort in the past few years has been focused on the spatial solitons in photorefractive (PR) materials. Since their prediction,[1] three different types of spatial solitons have been observed: the quasi-steady-state solitons,[1,2] the photovoltaic solitons,[3,4] and the screening solitons.[5,6] In general, spatial solitons are based on nonlinear changes of the refractive index induced by a propagating light beam. The beam propagates with an unchanging profile if the beam diffraction is exactly compensated by the refractive-index variation. Photovoltaic solitons occur in media with strong photovoltaic currents, where these currents lead to self-focusing.[7] Screening solitons emerge if the light beams of appropriate wavelength, intensity, and shape[8–10] are launched into a PR crystal, and a dc electric field is applied in the lateral direction, to induce the self-focusing of beams by PR screening. Quasi-steady-state solitons appear during the slow transient screening process.

Spatial solitons in PR media do not fulfill the formal mathematical definition of solitons, even if they propagate as a solitary wave with an unchanging beam profile. It is well known that solitons in integrable systems behave as particles; in particular, they preserve the shape after collisions. Typical examples are one-dimensional solitons in Kerr media.[11] In PR materials spatial solitons can interact inelastically, as we shall see later on. The term spatial soliton is used in a broader sense to describe nondiffracting self-trapped laser beams.[9,12]

The PR effect allows for self-trapping in one and two transverse dimensions at very low optical power levels (microwatts).[13,14] Both one-dimensional and two-dimensional (2D) spatial solitons have a unique shape, which is determined by the intensity, the strength of the external field, and the beam diameter.[8–10] However, the situation with the 2D solitons is more complicated. The self-focusing in two dimensions is anisotropic, which is caused by the external field being applied along one transverse direction. This anisotropy does not allow for circularly symmetric solitons. The overall structure of the index modulation produces solitons that are squeezed in the direction of the applied field. The squeezing need not be pronounced in an experiment. In addition, as it has been shown recently,[15] the beam-profile deviation from the exact 2D soliton shape causes oscillation of the beam's transverse diameters. The commonly used circularly symmetric Gaussian input beams are particularly affected. This has repercussions on the interaction of beams. Thus the proper analysis of screening solitons requires three spatial dimensions and time.

Owing to their stability in two dimensions and the existence at low power levels, PR spatial screening solitons seem very promising for all-optical applications, such as the soliton-induced guiding or switching. The idea is based on the fact that the spatial soliton is a fundamental mode of the waveguide it creates.[16,17] These waveguides can be easily controlled and can form complex structures, such as the X and Y junctions.[18–20] Because the PR effect is wavelength dependent, the spatial solitons can guide much more intense beams at less photosensitive wavelengths.[21] In general, nontrivial optical devices can make use of more than one spatial soliton; thus there is a need to analyze the interaction and mutual influence of two or more solitons in a PR crystal. Under certain conditions, coupled soliton pairs can be formed,[22–24] where the undistorted propagation of one beam depends on the presence of the other, and vice versa.

The inelastic character of soliton collision and interaction gives rise to a variety of interesting phenomena. Mutually incoherent PR spatial solitons display behavior similar to the solitons in saturable Kerr media.[25–27] Incoherent solitons are supported by a PR material because

of its slow response. The relative phase between two incoherent beams is assumed to vary on a time scale much faster than the medium response to the temporal interference pattern of beams. After a collision, incoherent solitons can keep their identity and remain unchanged, or exchange their identities, or form a bound state, or fuse into a single beam. Until now, we have not succeeded in handling these problems by analytical methods. For different physical systems such as optical fibers and quadratic media there exist some analytical approaches to describe the interaction of solitons.[28–31]

Recently the spiraling and the anomalous interaction of incoherent solitons have been observed experimentally.[32–34] For the isotropic PR nonlinearity a theory of stable soliton spiraling has been developed.[35] The mutually incoherent solitons can become partially coherent owing to a periodic power exchange while interacting. This leads to a dynamical stabilization of the spiraling. The phenomenon of induced coherence should not be restricted to spiraling interactions but should be a general feature of closely interacting self-guided beams. Depending on the interaction case, the power exchange should be more or less pronounced. However, in case of the anisotropic PR nonlinearity discussed in this paper, the situation is more complicated. Additional attractive and repulsive effects have to be considered owing to the anisotropic modulation of the refractive index. Nevertheless, for closely interacting solitons, energy-transfer processes are observed.

We perform a numerical analysis of the interaction of bright spatial screening solitons. Two beams are launched into a PR crystal and their interaction properties are studied by recording of the field distribution and trajectories of the propagating beams as functions of the propagation distance. The strong influence of the anisotropic character of the refractive-index modulation is displayed by choice of different initial launching positions and angles of the two beams in the transverse plane.

Section 2 of the paper contains the formulation of the model, Section 3 deals with the interaction of solitons, and Section 4 presents conclusions.

2. MODEL

A. Paraxial-Beam Propagation

The propagation of an optical beam inside a PR crystal can be described by the standard wave equation in paraxial approximation.[12] As one has more than one beam to contend with, the standard equation has to be modified to take the drift terms into account. The beams may propagate in different directions; each beam then defines its own paraxial-propagation axis, and the slowly varying envelope wave equation for each of the beams must be transformed to a common coordinate system, which is reasonably attached to the crystal. The modified propagation equation for the slowly varying envelope of the beam's electric field has the form

$$2ikn_0\partial_z\mathbf{A} + \nabla^2\mathbf{A} + 2ikn_0(\boldsymbol{\theta}\cdot\nabla)\mathbf{A} + k^2(\hat{n}^2\mathbf{A} - n_0^2\mathbf{A}) = 0, \quad (1)$$

where the envelope $\mathbf{A}(x, y, z)$ propagates in the z direction, with the vacuum wave number k. The operator ∇ is the transverse gradient, n_0 is the unperturbed refractive index of the crystal, and $\hat{n}^2 = \hat{n}^2(|A(x, y, z)|^2)$ is the refractive-index tensor induced by the propagating beam. The vector $\boldsymbol{\theta}$ specifies the launching angles of the beam. The components of $\boldsymbol{\theta}$ are the direction cosines of the launching direction.

The PR crystal responds to the presence of an optical field by a nonlinear change in the refractive index. The redistribution of photoexcited charges induces a space-charge electric field that screens out an externally applied dc electric field. The electric field inside the crystal changes the refractive index by means of the linear electro-optic effect: $n_{ij}^2 = n_0^2 + n_0^4\Sigma_k r_{ijk}\partial_k\phi$. Here r_{ijk} is the linear electro-optic tensor and $\partial_k\phi$ are the components of the space-charge field. The induced modulation of the refractive index has positive and negative parts, which lead to focusing and defocusing, respectively. Roughly speaking, the refractive index is increased in the region illuminated by the beam, whereas in the adjoining regions along the direction of the external field the refractive index is decreased.[15,36,37] Because the modulation of the refractive index is directly proportional to the induced space-charge field, the central positive parts of the index modulation are caused by the negative parts of the induced space-charge field, and the adjoining negative parts of the refractive index correspond to the positive tails of the space-charge field.

Numerical simulation is performed for a strontium barium niobate crystal. The incident beams are linearly polarized along the c axis to make use of the dominant r_{33} electro-optic coefficient. The external field is also applied along the c axis, perpendicular to the propagation direction. We assign conveniently the x axis of our physical coordinate system to the c axis and the z axis to the propagation direction. The (x, y) plane is then the transverse plane in which much of the action takes place. Under these assumptions, the propagation equation simplifies to a scalar partial differential equation. Because typical propagation distances are of the order of millimeters and typical beam diameters are of the order of micrometers, we introduce transverse and longitudinal scaling. The transverse-scaling length w is typically of the order of beam diameter, and the propagation-scaling length is accordingly determined by the diffraction length $L_D = kn_0w^2$. After some algebra, the propagation equation is transformed into a dimensionless form:

$$\partial_z A - \frac{i}{2}\nabla^2 A + \beta(\boldsymbol{\theta}\cdot\nabla)A = \frac{i\gamma}{2}\partial_x\phi A, \quad (2)$$

where $\beta = L_D/w$ is the scaling factor and $\gamma = k^2n_0^4w^2r_{33}$ is the PR coupling constant. For a given $\boldsymbol{\theta}$, the factors $\beta\theta_x$ and $\beta\theta_y$ give the shift of the beam (launched at the origin) along the x and y axes (in units of w) after a propagation distance of L_D.

B. Potential Equation

The space-charge field can be obtained from the band-transport model of Kukhtarev *et al.*[38,39] The standard set of equations for electrons as the sole charge

carriers[8–10,36] is written in a slightly different way, with the potential ϕ of the space-charge field $\mathbf{E}_{sc} = -\nabla\phi$:

$$\partial_t N_D^+ = S_i(I_{sat} + I)(N_D - N_D^+) - S_r n N_D^+, \quad (3a)$$

$$e(\partial_t n - \partial_t N_D^+) = -\nabla \mathbf{j}, \quad (3b)$$

$$\mathbf{j} = \mu e n \nabla\phi + \mu k_B T \nabla n, \quad (3c)$$

$$\epsilon_0 \epsilon_r \nabla^2 \phi = e(N_D^+ - N_A - n). \quad (3d)$$

In these equations, N_D is the donor concentration, N_D^+ is the density of ionized donors, N_A is the acceptor density, and n is the free-electron density. e and μ stand for the electronic charge and mobility. S_i is the photoexcitation cross section, and S_r is the charge-carrier recombination rate. k_B is Boltzmann's constant, T is the absolute temperature, ϵ_r is the scalar dielectric constant of the medium, and $\mathbf{j}$ is the current density.

The total intensity of the propagating beam is given by $I(x, y, z) = |A(x, y, z)|^2$. The so-called saturation intensity $I_{sat} = I_{th} + I_B$ includes additional contributions to the concentration of ionized donors, written in terms of different intensities.[15] Here the intensity owing to thermally generated charge carriers and the intensity owing to the experimental background illumination are taken into account.[9] I_{th} is very small compared with I and I_B. In what follows the physical intensity of the propagating beam is normalized to the saturation intensity and the photoexcitation cross section is appropriately modified: $S_i(I_{sat} + I)$ is replaced by $S_i(1 + I)$.

In PR media the concentration of ionized donors approximately equals the concentration of acceptors: $N_D^+ \approx N_A$. Inserting this approximation in the steady-state Eq. (3a), one obtains an expression for the free-electron density n in terms of light intensity:

$$n = \frac{S_i(1 + I)(N_D - N_A)}{S_r N_A}. \quad (4)$$

On the other hand, substituting Eqs. (3d) and (3c) into Eq. (3b) yields a time-dependent potential equation for the space-charge field:

$$\epsilon_0 \epsilon_r \partial_t(\nabla^2\phi) - \mu e n \nabla^2\phi - \mu e \nabla n \nabla\phi - \mu k_B T \nabla^2 n = 0. \quad (5)$$

Because the spatial screening solitons are observed only if a dc external electric field is applied, we introduce the electrostatic potential induced by the light: $\tilde{\phi} = \phi + E_0 x$. With such a choice the incorporation of boundary conditions is easy: $\tilde{\phi}(x, y, z) \to 0$ for $x, y \to \infty$. Incorporating Eq. (4) into Eq. (5), and after some rearranging, one finds the intensity-dependent potential equation:

$$\tau\partial_t(\nabla^2\tilde{\phi}) - \nabla^2\tilde{\phi} - \nabla \ln(1 + I)\nabla\tilde{\phi} = -E_0 \partial_x \ln(1 + I) + \frac{k_B T}{e}\{\nabla^2 \ln(1 + I) + [\nabla \ln(1 + I)]^2\}, \quad (6)$$

where

$$\tau = \frac{\epsilon_0 \epsilon_r S_r N_A}{\mu e S_i (1 + I)(N_D - N_A)} \quad (7)$$

is the intensity-dependent relaxation time of the crystal. The first term on the right side of Eq. (6) is due to the drift of charge carriers in the electric field. If there is no external field, then there are no screening solitons. The last term on the right side comes from the diffusion field of the crystal. The charge-carrier diffusion causes the beams to bend, similar to the bending found in one dimension.[40] This effect can be controlled by adjustment of the absolute temperature T. The potential equation (6) and the paraxial propagation equation for the beam [Eq. (2)] form the basic set of equations for our model.

3. INTERACTION OF TWO PROPAGATING BEAMS

The interaction behavior of two propagating bright spatial screening solitons in a PR crystal is analyzed by numerical simulation of the model equations. The slowly varying amplitudes $A_1(x, y, z)$ and $A_2(x, y, z)$ obey the following paraxial-propagation equations:

$$\partial_z A_1 - \frac{i}{2}\nabla^2 A_1 + \beta(\boldsymbol{\theta}_1 \cdot \nabla)A_1 = \frac{i\gamma}{2}\partial_x \phi A_1, \quad (8a)$$

$$\partial_z A_2 - \frac{i}{2}\nabla^2 A_2 + \beta(\boldsymbol{\theta}_2 \cdot \nabla)A_2 = \frac{i\gamma}{2}\partial_x \phi A_2. \quad (8b)$$

The response of the PR crystal to the presence of optical fields is calculated by the potential equation (6). In this paper we consider only the steady state, $\tau\partial_t(\nabla^2\tilde{\phi}) = 0$. Also, the diffusion-field effects are neglected ($T = 0$). In the case of incoherent beams the total intensity distribution is given by $I(x, y, z) = |A_1(x, y, z)|^2 + |A_2(x, y, z)|^2$. The propagation equations are solved by a modified beam-propagation method,[41,42] and the potential equation is treated by the Crank–Nicholson finite-difference scheme. The treatment of the time-dependent case requires an additional temporal integration loop.

Initially Gaussian beams are launched into the crystal,

$$A_1(x, y, 0) = A_1^0 \exp\left[-\frac{(x - x_1)^2}{\sigma_x^2} - \frac{(y - y_1)^2}{\sigma_y^2}\right], \quad (9a)$$

$$A_2(x, y, 0) = A_2^0 \exp\left[-\frac{(x - x_2)^2}{\tilde{\sigma}_x^2} - \frac{(y - y_2)^2}{\tilde{\sigma}_y^2}\right], \quad (9b)$$

where A_1^0 and A_2^0 are the normalized initial amplitudes of the beams, and σ's are the initial $1/e$ diameters in the x and y directions. Input positions in the transverse plane are given by the coordinate pairs (x_1, y_1) and (x_2, y_2). The origin of the coordinate system is chosen to be the center of mass of the initial intensity distribution of the two beams.

The values of all simulation parameters are chosen consistently with the common experimental values.[32] A typical strontium barium niobate crystal allows for a propagation distance of a few millimeters (here taken as $L_z = 6.5$ mm), its electro-optic coefficient is $r_{33} = 180$ pm/V, and the unperturbed refractive index is $n_0 = 2.35$. The wavelength of the propagating beams is $\lambda = 488$ nm. Two circular Gaussian beams with $w = 12\,\mu$m FWHM spot size are launched into the crystal.

Their half 1/*e* width $\sigma = 0.5988$ (in dimensionless units) corresponds directly to the diameters in Eq. (9). The photorefractive coupling constant is $\gamma = 9.775 \times 10^{-3}$ cm/V. An external field of $E_0 = 4357$ V/cm is applied across the crystal.

Because the electric field is directed along the *x* axis, the spatial symmetry in the transverse plane is broken. In this paper we study the consequences of this anisotropy on the steady-state interaction behavior of two beams launched either parallel or perpendicular or skewed in the direction of the external field.

A. Parallel Orientation

First, we consider the interaction of two beams launched in parallel, with the initial positions along the *x* axis. The beams propagate in the *z* direction. As it is known,[33] the incoherent spatial solitons in PR media exhibit an anomalous interaction behavior along the direction of the external field. If the initial beam separation is of the order of the beam diameter or smaller, the beams attract each other and eventually merge. On the other hand, if the distance is larger than the diameter, the beams repel. These effects result from the long-range anisotropic nature of the induced space-charge field.

Another consequence of the anisotropy can be used to present the propagation dynamics of the interacting beams in detail. If the beams are launched separated in parallel to the external field, the beams stay on the *x* axis and remain confined to the (x, z) plane. To present the trajectories of the solitons it is sufficient to record the transverse intensity distribution along the *x* axis ($y = 0$) during propagation. The reason for this will become clear in the following section.

Figure 1 depicts the intensity distributions of propagating beams for four different initial separations. In Fig. 1a the normalized initial separation is $\Delta x = 0.9$. The initial distance is smaller than the beam FWHM, and the beams overlap strongly. This increases the refractive index in between and, as a consequence, the beams attract and merge. When the beams propagate quite close for longer distances, they lose the original shape and experience periodic changes in amplitude and profile. However, their trajectories are still well defined. Although they overlap almost completely, they spatially oscillate about the *z* axis. Such a propagation resembles a single beam that periodically changes its beam characteristics.

In Fig. 1b the initial distance is increased to $\Delta x = 1.0$. Close to the input face, beams still overlap, and the refractive index in between them is increased. This results in an initial attraction. Because the shape of the input beams is Gaussian, the beam profile oscillates in both transverse directions during propagation.[15] The diameters of the beams also decrease. This transient reduction of diameters is faster than the reduction of the distance between beams, so the attraction changes into repulsion because both beams gradually feel more of the repulsive tails of the other beam's space-charge field. A further increase of the initial distance leads to an immediate repulsion.

If the shape of each of the launched beams matches the characteristic soliton shape, it should be possible to observe a bound state, where the beams neither attract nor repel each other. This is not observed for the Gaussian input beams. In Figs. 1c and 1d the interaction behavior for initial configurations close to the bound state are shown; in Fig. 1c the beams are initially separated by $\Delta x = 0.966$ and in Fig. 1d by $\Delta x = 0.967$. In both cases the beam separation does not change for nearly 1.5 diffraction lengths and the beams propagate in a quasi bound state, but finally they attract or repel each other, respectively, owing to the internal oscillations. More precise adjustments of initial separation will lead to extended unperturbed propagations but will not avoid final attraction or repulsion. The details of the quasi-bound-state propagation, especially the role of the still overlapping and interacting electric fields of the beams, and additional influences owing to induced coherence are subject to present investigations.

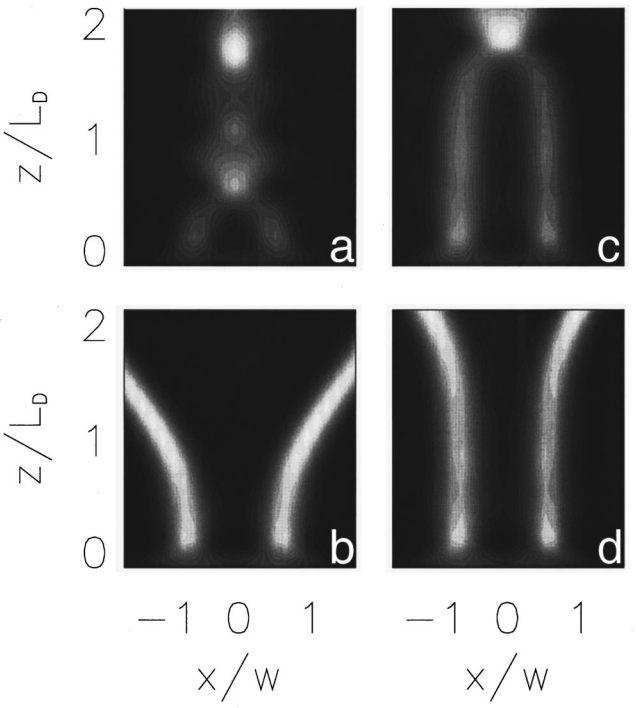

Fig. 1. Interaction of incoherent beams launched on the *x* axis. The normalized propagation distance is 2. The initial separations are (a) 0.9, (b) 1.0, (c) 0.966, and (d) 0.967. The normalized input intensity is 1.5.

Interaction of beams launched separated along the *x* axis is determined not only by the beams' initial distance but also by the input intensity. Figure 2 displays intensity distributions along the *x* axis for three different initial separations and three different intensities. In the left column, beams are launched separated by $\Delta x = 0.4$. In all cases beams attract each other and merge. The lower the intensity, the stronger the damping of the spatial oscillation about the *z* axis. For an initial intensity of 1.5 [Fig. 2a] this oscillation dies away after propagating approximately one diffraction length, and the beams merely experience diameter oscillations. In contrast, beam intensities of 3.5 and 5.5, as shown in Figs. 2b and 2c, respectively, lead to slightly damped or periodic oscillations.

An initial separation of $\Delta x = 1.0$ results in an immediate repulsion of the beams. In Figs. 2g–2i the normal-

ized launching intensities are again 1.5, 3.5, and 5.5, respectively. Higher beam intensities cause stronger shape oscillations but not stronger interaction in general. Because the final separation between beams propagating for two diffraction lengths is higher if the intensity is increased from 1.5 to 3.5 than from 3.5 to 5.5, the influence of shape oscillations on the repulsion is negligible. The interaction reaches a steady state; here the saturable character of the photorefractive nonlinearity comes into play.

In the attracting (Figs. 2a–2c) and repelling (Figs. 2g–2i) cases discussed so far, the intensity dependence of the interaction is of minor importance. However, a qualitative change can be observed, if the initial beam separation is chosen to be $\Delta x = 0.7$. As shown in Fig. 2d, the beams simply attract and carry out damped oscillations about the z axis. If the intensity is increased to 3.5 (Fig. 2e) the two beams attract each other immediately as they enter the crystal. But after collision, the beams separate from each other and propagate individually for a certain distance until they attract, collide, and separate again. The following separations are less pronounced, and finally the beams show the already-discussed damped oscillations.

In contrast, if the input intensity exceeds a certain value, as for 5.5 in Fig. 2f, the beams repel each other after the first collision. If the internal shape oscillations—owing to the collision and the Gaussian shape of the input beams—and the connected diameter reductions exceed the reduction of the beam separation, then each beam feels the repulsive tail from the other beam and they repel each other. This is a completely new interaction case: beams repel although they are launched rather close to each other. It could be shown that the beams exchange their position after the collision.

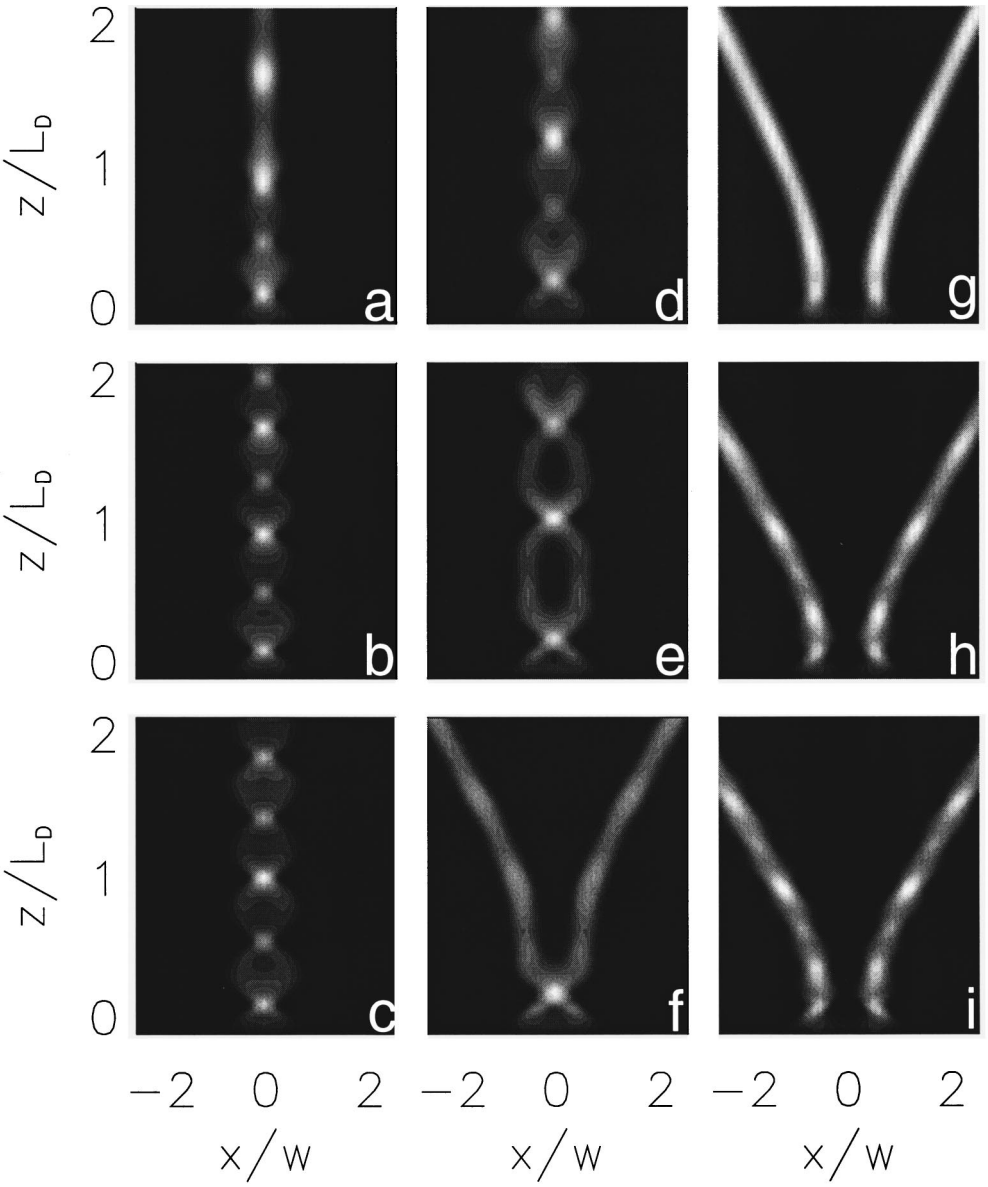

Fig. 2. Interacting incoherent beams for three different launching intensities and three different initial separations. The normalized intensity increases from 1.5 in the upper row, to 3.5 in the middle, to 5.5 in the bottom row. The normalized separation is 0.4 (left column), 0.7 (middle column), and 1.0 (right column). The beams propagate for two diffraction lengths.

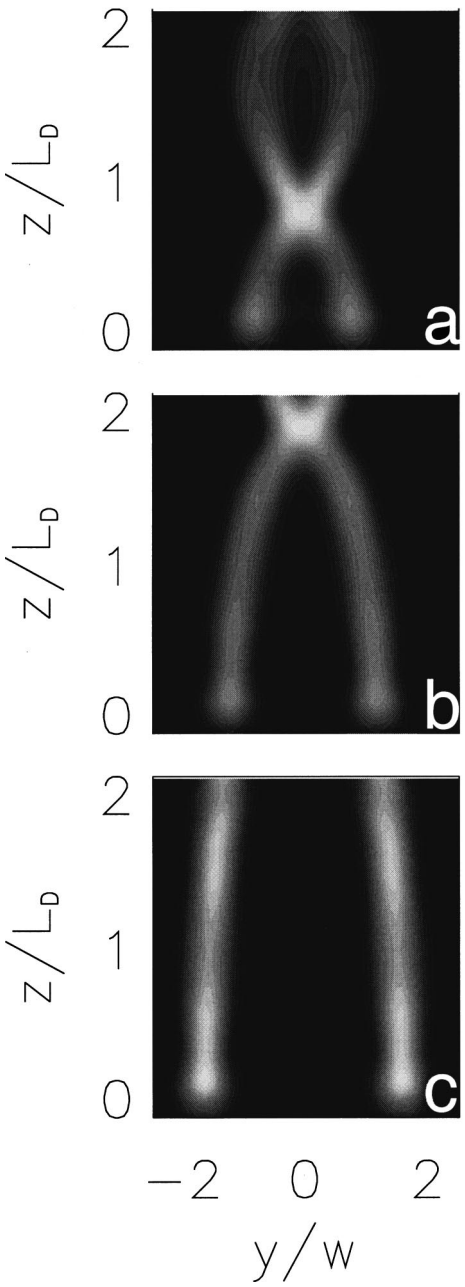

Fig. 3. Intensity distributions for two interacting incoherent beams, launched separated along the *y* axis. The normalized separations are (a) 1.6, (b) 2.4, and (c) 3.2. The normalized input intensity is 1.5.

B. Perpendicular Orientation

In the following discussion, incoherent beams are launched along the *y* axis, perpendicular to the direction of the external field. Figures 3a–3c show the intensity distribution along the *y* axis for different initial separations. In all cases the solitons attract each other. The fundamental propagation features are similar to those of the attracting beams launched along the *x* axis. However, there is an important difference. Owing to the anisotropy of the induced space-charge fields, the repulsive tails do not exist in the *y* direction. The refractive-index modulation decays monotonically to zero. As a consequence only attraction is observable for incoherent beams. The strength of the attraction is mainly determined by the distance between the beams and does not qualitatively change with different intensities. This behavior is essentially the same as the one found in isotropic self-focusing media.

Both the solitons launched separated along the *x* axis and the solitons launched separated along the *y* axis remain on their respective axes in the course of propagation. Solitons attract each other in the perpendicular direction. Perpendicular repulsion is not observed; hence the beams remain positioned in the launching plane. The situation changes drastically for skewed launching relative to the direction of the external field.

C. Influence of Angular Separation

The common feature of results presented above is that the beams are launched in parallel, perpendicular to the transverse plane. In this subsection we study the influence of the initial angular separation of the beams on the interaction behavior. To demonstrate the difference, we start from an already-discussed case 1, two incoherent beams launched separated along the direction of the external field.

When tilted beams are launched, three different regimes are observed. In Fig. 4, the initial separation of $\Delta x = 1.0$ results in repulsion of the parallel propagating beams (Fig. 4a). For small input angles the situation does not change. The repulsive tails of the induced space-charge fields cannot be compensated for by the convergence of the beam trajectories. Increasing the input angle to $\theta_x = -0.5$ leads to the second regime, as shown in Fig. 4b. The beams come closer to each other, and the overlap of the optical fields prevents the emergence of the repulsive tails. The beams fuse in the end, owing to attraction. The third regime is reached if the input angle is $\theta_x = -0.75$ (Fig. 4c). The reduction of the initial beam separation is dominated by the convergence of their trajectories. The beams collide, cross each other, and fly apart because the mutual attraction cannot compensate for the strong divergence of trajectories after collision. This effect is amplified by the repulsive interaction of the space-charge fields when the beams become sufficiently separated.

The presented observations are not limited to incoherent beams. In general, the attraction of two coherent or incoherent beams can always be compensated by a certain initial divergence of beam trajectories. Beam repulsion can be compensated by use of converging beam trajectories. For beams that match the soliton shape it should be possible to reach a stable equilibrium state.

D. Arbitrary Orientation

For arbitrary launching positions in the transverse plane one generally observes the mutual rotation of beams. There exists the region of attraction around the origin in the transverse plane that is about the size of two FWHM beam spot sizes along the *x* axis and extends indefinitely along the *y* axis. The whole *y* axis and the attractive portion of the *x* axis are the stable directions for the propagation of incoherent solitons. Launched anywhere within the attractive region, but symmetrically about the origin, the beams initially rotate around the *z* axis and

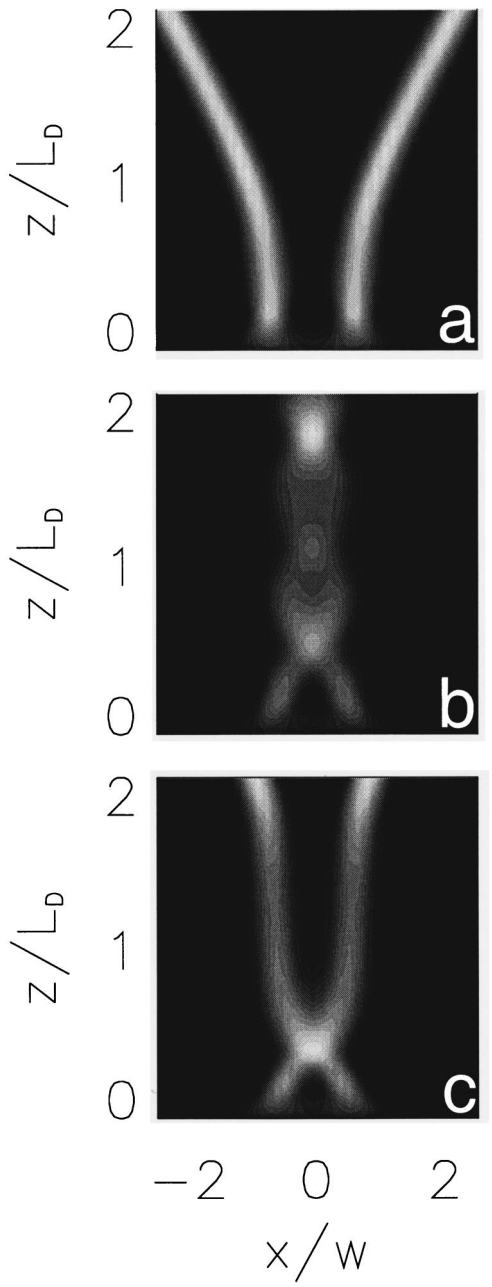

Fig. 4. Interaction of tilted incoherent beams. The trajectories of the beams in the plane (x, z) are shown. The beams propagate (a) in parallel, and the beams are tilted in the x direction for (b) -0.5, and (c) -0.75. The tilt along the y direction is zero. The normalized input intensity is 1.5.

approach each other. As they come close, they start interacting strongly and perform various "dancing acts" in the plane. Because the beams propagate quite close for a long distance, induced coherence of the beams supports the interaction.

Examples of such motion are displayed in Fig. 5, for three different launching orientations: close to the x axis (15°), close to the y axis (75°), and in between (45°). To demonstrate the influence of three different input intensities, the transverse intensity distribution at the output face is shown for each launching configuration. The beams are initially separated by 1.5 and propagate for two diffraction lengths.

When launched close to the x axis (Fig. 5a), the beams repel each other (Figs. 5b–5d) and increase their separation. The interaction resembles the repulsive on-axis behavior discussed above and is dominated by the repulsive tails of the induced space-charge fields. But there is an important difference. Owing to the transverse shift along y, the repulsive tails emerge shifted. This results in a strong repulsive force along y, which exceeds the force along x. The beams repel almost perpendicular to the direction of the external field. The interaction is weakly dependent on the beam intensity.

The character of the interaction changes, if the input beams are skewed by 45° (Fig. 5e). The transverse distance along x is smaller, and the attractive regions of the space-charge fields cause an attraction along x. Owing to the anisotropy of the induced space-charge fields, the forces along the direction of the external field still dominate the interaction. This should finally result in damped oscillations about the y axis, until the beams finally attract along y and merge. However, the transient beam-diameter oscillations of the Gaussian input beams come into play again. The initial attraction along x changes into repulsion before the turning point of the spatial beam oscillation is reached. Owing to the beam-diameter reductions, the emerging repulsive tails cannot be compensated, and the beams fly apart (Figs. 5f–5h). This effect is strongly dependent on the beam intensity, because the shape of the induced space-charge fields is dependent on the slope of the intensity distribution.

Beams launched close to the y axis (Fig. 5i) are subjected to the attraction along y. Although there are slight spatial oscillations along x that are observed (Figs. 5k–5m), the beams do not leave the attractive region and head toward the central region. When viewed along the z axis, the motion sometimes resembles spiraling, and sometimes it resembles simple oscillation along the x and y axes, but generally it is more complicated than that. The pair of solitons twists and turns about the z axis in a damped motion and eventually fuses into one beam.

The observation of simple spiraling, as reported in Ref. 32, requires rather precise shooting. The long attractive well along the y axis always breaks symmetry and induces elongated orbits. One has to carefully pick the initial positions for perpendicular launching and then adjust with the tilts to produce long-lasting spiraling. The spiraling behavior has been analyzed in more detail elsewhere.[43,44] However, such motion cannot persist for long. In the end the solitons will either fuse or fly apart. It should be mentioned that when the solitons are close to each other and interact strongly, they entangle and their individual identities are rather dubious. The light-intensity distributions do not show two distinct beams anymore. However, as soon as the beams disentangle, two bright spots reappear.

4. CONCLUSIONS

We have investigated the interaction of spatial screening solitons in a PR crystal. Soliton propagation is governed by the spatial modulation of the medium's refractive index induced by both beams. Because the induced space-charge field and the corresponding total refractive-index modulation are anisotropic, the interaction behavior is for

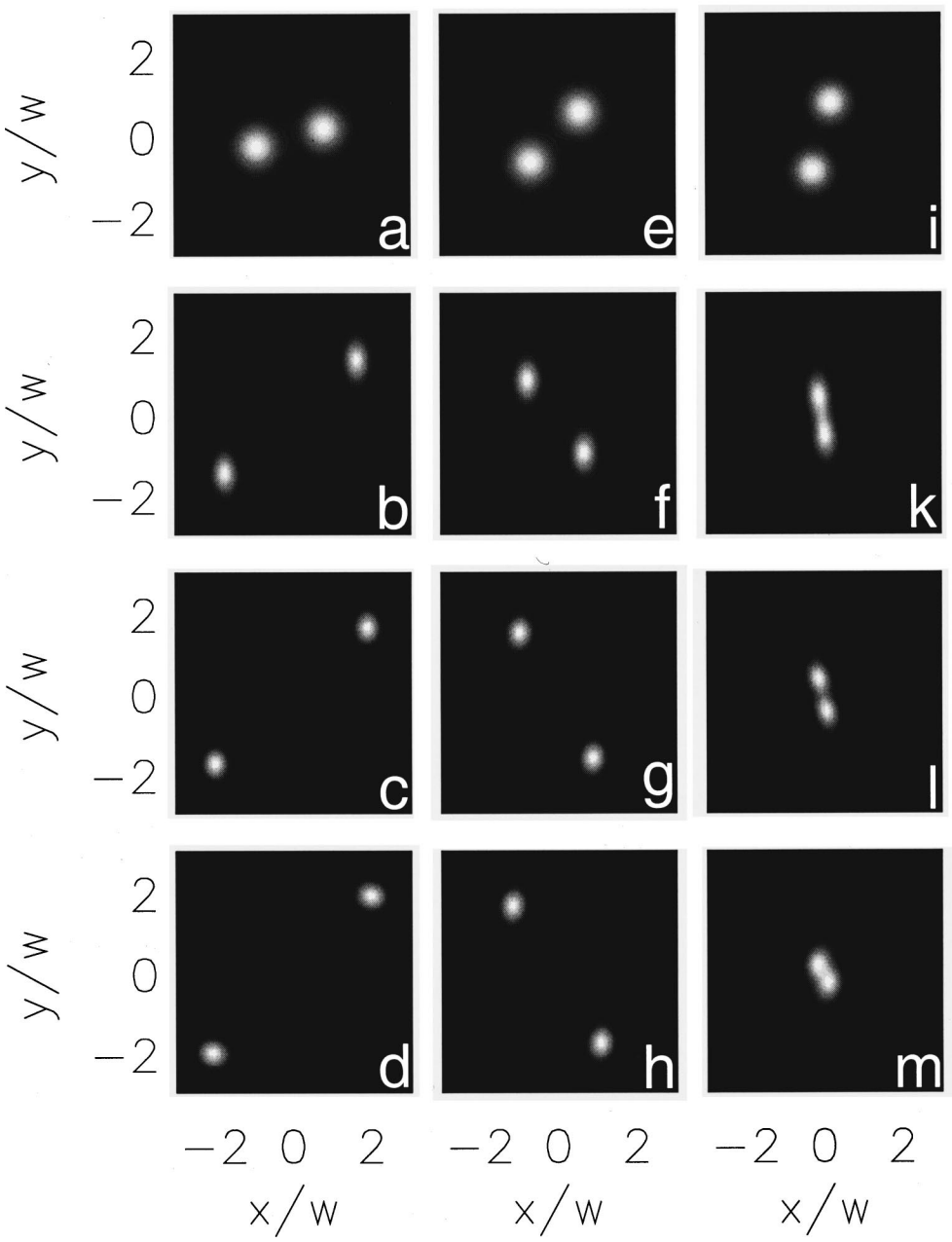

Fig. 5. Interaction of arbitrarily oriented solitons. Transverse intensity distributions at the input face of the crystal are displayed in the top row for three different pairs of solitons, initially skewed by (a) 15°, (e) 45°, and (i) 75°. The output face of the crystal is shown for three different input intensities: 1.0 in the second row, 3.0 in the third, and 5.0 in the bottom row. All pairs propagate for two diffraction lengths; their initial separation is 1.5.

the most part determined by the geometrical arrangement of beams in the transverse input plane. In particular, the beam separation plays an important role. If the incoherent beams are initially positioned along the direction of the applied field, then they display the recently discovered anomalous behavior. They repel each other if a certain initial separation is exceeded; otherwise they attract and fuse into a single beam. Incoherent beams initially placed along the *y* axis, i.e., perpendicular to the external field, always show attraction, similar to what is expected for solitons in saturable media.

Incoherent beams propagating very close to each other can exchange energy. The effects of this induced coherence cause additional attractive or repulsive forces, leading, for example, to a dynamical stabilization of the spiraling motion in case of the isotropic PR nonlinearity.[35]

We observe spatial propagation phenomena that are caused by the use of Gaussian beams. Such beams do not match the exact soliton shape and suffer initial transient beam-diameter reduction, followed by the oscillation of diameters. These effects influence the interaction behavior, and we have found that initial attraction can change into repulsion during propagation.

Additional effects can be caused by the input intensity. A certain geometrical arrangement of the input beams leading to attraction for low-intensity beams can change into a combination of position exchange and repulsion if the intensity is increased.

The attraction and repulsion are influenced by the initial tilt of beams launched into the crystal. The divergence and the convergence of the beam trajectories can compensate for attraction and repulsion.

The study of on-axis interaction of the beams allows for deeper understanding of the basic mechanisms of attraction and repulsion, which can lead to a more complex behavior, such as spiraling. The off-axis launching in combination with the initial angular tilt makes the spiraling and the oscillatory interaction behavior possible. The beams perform complicated motion in the transverse plane, rotating about the origin, twisting and turning in the region of attraction. Finally, they fuse. We find that the interaction between incoherent screening solitons is basically anisotropic, which may not be apparent in the early stages of soliton propagation.

In the end, a few comments are in order. First, we presented only the steady-state propagation and excluded the diffusion field, even though our code is capable of capturing the dynamical and the drift effects. We wanted to expose clearly the steady-state picture of soliton propagation. Second, it is interesting to construct a dynamical theory of interacting 2D solitons, considering them as quasi particles. Such a theory cannot be a pure mechanical theory of "orbiting" and "repelling" solitons, as electrical effects are playing a prominent role. It also cannot be a pure electromechanical theory, as light and the PR effect play an important role.

Another interesting extension is to consider the interaction of more than two solitons and the types of structures they could build in the transverse plane. It is conceivable that the questions of the stability of transverse patterns, as well as the appearance of defects ("birth and death" of solitons) would come to the fore.

ACKNOWLEDGMENTS

Research at the Darmstadt University of Technology is supported by the Deutsche Forschungsgemeinschaft. M. Belic acknowledges financial support within the Sonderforschungsbereich 185. We would like to thank Oliver Sandfuchs for valuable discussions.

REFERENCES

1. M. Segev, B. Crosignani, A. Yariv, and B. Fischer, "Spatial solitons in photorefractive media," Phys. Rev. Lett. **68**, 923–926 (1992).
2. G. Duree, J. L. Shultz, G. Salamo, M. Segev, A. Yariv, B. Crosignani, P. DiPorto, E. Sharp, and R. Neurgaonkar, "Observation of self-trapping of an optical beam due to the photorefractive effect," Phys. Rev. Lett. **71**, 533–536 (1993).
3. G. C. Valley, M. Segev, B. Crosignani, A. Yariv, M. M. Fejer, and M. Bashaw, "Dark and bright photovoltaic spatial solitons," Phys. Rev. A **50**, R4457–R4460 (1994).
4. M. Taya, M. Bashaw, M. M. Fejer, M. Segev, and G. C. Valley, "Observation of dark photovoltaic spatial solitons," Phys. Rev. A **52**, 3095–3100 (1995).
5. M. D. Iturbe-Castillo, P. A. Marquez-Aguilar, J. J. Sanchez-Mondragon, S. Stepanov, and V. Vysloukh, "Spatial solitons in photorefractive $Bi_{20}TiO_{20}$ with drift mechanism of nonlinearity," Appl. Phys. Lett. **64**, 408–410 (1994).
6. M. Segev, G. C. Valley, B. Crosignani, P. DiPorto, and A. Yariv, "Steady-state spatial screening solitons in photorefractive materials with external applied field," Phys. Rev. Lett. **73**, 3211–3214 (1994).
7. M. Segev, G. C. Valley, M. C. Bashaw, M. Taya, and M. M. Fejer, "Photovoltaic spatial solitons," J. Opt. Soc. Am. B **14**, 1772–1781 (1997).
8. D. N. Christodoulides and M. J. Carvalho, "Bright, dark, and gray spatial soliton states in photorefractive media," J. Opt. Soc. Am. B **12**, 1628–1633 (1995).
9. M. Segev, M. Shih, and G. C. Valley, "Photorefractive screening solitons of high and low intensity," J. Opt. Soc. Am. B **13**, 706–718 (1996).
10. B. Crosignani, P. DiPorto, A. Degasperis, M. Segev, and S. Trillo, "Three-dimensional optical beam propagation and solitons in photorefractive crystals," J. Opt. Soc. Am. B **14**, 3078–3090 (1997).
11. V. E. Zakharov and A. B. Shabat, Zh. Eksp. Teor. Fiz. **61**, 118 (1971); "Exact theory of two-dimensional self-focusing and one-dimensional self-modulation of waves in nonlinear media," Sov. Phys. JETP **34**, 62–69 (1972).
12. A. W. Snyder and Y. S. Kivshar, "Bright spatial solitons in non-Kerr media: stationary beams and dynamical evolution," J. Opt. Soc. Am. B **14**, 3025–3031 (1997).
13. M. Shih, M. Segev, G. C. Valley, G. Salamo, B. Crosignani, and P. DiPorto, "Observation of two-dimensional steady-state photorefractive screening solitons," Electron. Lett. **31**, 826–827 (1995).
14. M. Shih, P. Leach, M. Segev, M. H. Garrett, G. Salamo, and G. C. Valley, "Two-dimensional steady-state photorefractive screening solitons," Opt. Lett. **21**, 324–326 (1996).
15. A. A. Zozulya, D. Z. Anderson, A. V. Mamaev, and M. Saffman, "Solitary attractors and low-order filamentation in anisotropic self-focusing media," Phys. Rev. A **57**, 522–534 (1998).
16. M. Shih, M. Segev, and G. Salamo, "Circular waveguides induced by two-dimensional bright steady-state photorefractive spatial screening solitons," Opt. Lett. **21**, 931–933 (1996).
17. M. Shih, Z. Chen, M. Mitchell, M. Segev, H. Lee, S. Feigelson, and J. P. Wilde, "Waveguides induced by photorefractive screening solitons," J. Opt. Soc. Am. B **14**, 3091–3101 (1997).
18. B. Luther-Davies and X. Yang, "Waveguides and Y junctions formed in bulk media by using dark spatial solitons," Opt. Lett. **17**, 496–498 (1992).
19. N. N. Akhmediev and A. Ankiewicz, "Spatial soliton X-junctions and couplers," Opt. Commun. **100**, 186–192 (1993).
20. W. Krolikowski and S. A. Holstrom, "Fusion and birth of spatial solitons upon collision," Opt. Lett. **22**, 369–371 (1996).
21. M. Morin, G. Duree, G. Salamo, and M. Segev, "Waveguides formed by quasi-steady-state photorefractive spatial solitons," Opt. Lett. **20**, 2066–2068 (1995).
22. D. N. Christodoulides, S. R. Singh, M. I. Carvalho, and M. Segev, "Incoherently coupled soliton pairs in biased photorefractive crystals," Appl. Phys. Lett. **68**, 1763–1765 (1996).
23. Z. Chen, M. Segev, T. H. Coskun, and D. N. Christodoulides, "Observation of incoherently coupled photorefractive spatial soliton pairs," Opt. Lett. **21**, 1436–1438 (1996).
24. Z. Chen, M. Segev, T. H. Coskun, D. N. Christodoulides, and Y. Kivshar, "Coupled photorefractive spatial soliton pairs," J. Opt. Soc. Am. B **14**, 3066–3077 (1997).
25. M. Shih and M. Segev, "Incoherent collisions between two-dimensional bright steady-state photorefractive spatial screening solitons," Opt. Lett. **21**, 1538–1540 (1996).
26. S. Gatz and J. Herrmann, "Soliton collision and soliton fusion in dispersive materials with a linear and quadratic intensity depending refraction index change," IEEE J. Quantum Electron. **28**, 1732–1738 (1992).
27. S. Gatz and J. Herrmann, "The propagation of optical beams and the properties of two-dimensional spatial solitons in media with a local saturable nonlinear refractive index," J. Opt. Soc. Am. B **14**, 1795–1806 (1997).
28. K. A. Gorshkov and L. A. Ostrovsky, "Interaction of solitons in nonintegrable systems: direct perturbation method and applications," Physica D **2**, 428–438 (1981).

29. D. J. Kaup, "Perturbation theory for solitons in optical fibers," Phys. Rev. A **42**, 5689–5694 (1990).
30. B. A. Malomed, "Polarization dynamics and interactions of solitons in a birefringent optical fiber," Phys. Rev. A **43**, 410–423 (1991).
31. A. V. Buryak and V. V. Steblina, "Soliton collisions in bulk quadratic media: analytical and numerical study," J. Opt. Soc. Am. B **16**, 245–255 (1999).
32. M. Shih, M. Segev, and G. Salamo, "Three-dimensional spiraling of interacting spatial solitons," Phys. Rev. Lett. **78**, 2551–2554 (1997).
33. W. Krolikowski, M. Saffman, B. Luther-Davies, and C. Denz, "Anomalous interaction of spatial solitons in photorefractive media," Phys. Rev. Lett. **80**, 3240–3243 (1998).
34. A. Stepken, F. Kaiser, M. R. Belić, and W. Krolikowski, "Interaction of incoherent two-dimensional photorefractive solitons," Phys. Rev. E **58**, R4112–R4115 (1998).
35. A. V. Buryak, Y. S. Kivshar, M. Shih, and M. Segev, "Induced coherence and stable soliton spiraling," Phys. Rev. Lett. **82**, 81–84 (1999).
36. A. A. Zozulya and D. Z. Anderson, "Propagation of an optical beam in a photorefractive medium in the presence of a photogalvanic nonlinearity or an externally applied electric field," Phys. Rev. A **51**, 1520–1531 (1995).
37. C. M. Gomez Sarabia, P. A. Marquez Aguilar, J. J. Sanchez Mondragon, S. Stepanov, and V. Vysloukh, "Dynamics of photoinduced lens formation in photorefractive $Bi_{12}TiO_{20}$ crystal under external DC electric field," J. Opt. Soc. Am. B **13**, 2767–2774 (1996).
38. N. V. Kukhtarev, V. B. Markov, S. G. Odulov, M. S. Soskin, and V. L. Vinetskii, "Holographic storage in electro-optic crystals. I. Steady-state," Ferroelectrics **22**, 949–960 (1979).
39. P. Yeh, *Introduction to Photorefractive Nonlinear Optics* (Wiley, New York, 1995).
40. M. I. Carvalho, S. R. Singh, and D. N. Christodoulides, "Self-deflection of steady-state bright spatial solitons in biased photorefractive crystals," Opt. Commun. **120**, 311–315 (1995).
41. M. Lax, G. P. Agrawal, M. R. Belić, B. J. Coffey, and W. L. Louisell, "Electromagnetic-field distribution in loaded unstable resonators," J. Opt. Soc. Am. A **2**, 731–742 (1985).
42. M. R. Belić, J. Leonardy, D. Timotijević, and F. Kaiser, "Spatiotemporal effects in double phase conjugation," J. Opt. Soc. Am. B **12**, 1602–1616 (1995).
43. A. Stepken, M. R. Belić, F. Kaiser, W. Krolikowski, and B. Luther-Davies, "Three dimensional trajectories of interacting incoherent photorefractive solitons," Phys. Rev. Lett. **82**, 540–543 (1999).
44. M. R. Belić, A. Stepken, and F. Kaiser, "Spiraling behavior of photorefractive screening solitons," Phys. Rev. Lett. **82**, 544–547 (1999).